SUPPLEMENTARY INFORMATION FOR

In situ generation, metabolism and immunomodulatory signaling actions of nitro-conjugated linoleic acid in a murine model of inflammation

Luis Villacorta[1,*], Lucia Minarrieta[2,3], Sonia R. Salvatore[4], Nicholas K. Khoo[4], Oren Rom[1], Zhen Gao[1], Rebecca C. Berman[1], Soma Jobbagy[4], Lihua Li[4], Steven R. Woodcock[4], Y. Eugene Chen[5], Bruce A. Freeman[4], Ana M. Ferreira[2], Francisco J. Schopfer[4] and Dario A. Vitturi[4,*].

[1]Department of Internal Medicine and [5]Department of Cardiac Surgery, Frankel Cardiovascular Center, University of Michigan Medical Center, Ann Arbor, MI, USA.; [2]Cátedra de Inmunología, Facultad de Química y Ciencias, Universidad de la República, Montevideo, Uruguay; [3]Institute of Infection Immunology, TWINCORE. Hannover, Germany; [4]Department of Pharmacology and Chemical Biology, University of Pittsburgh. Pittsburgh, PA, USA.

[*] Co-corresponding authors.

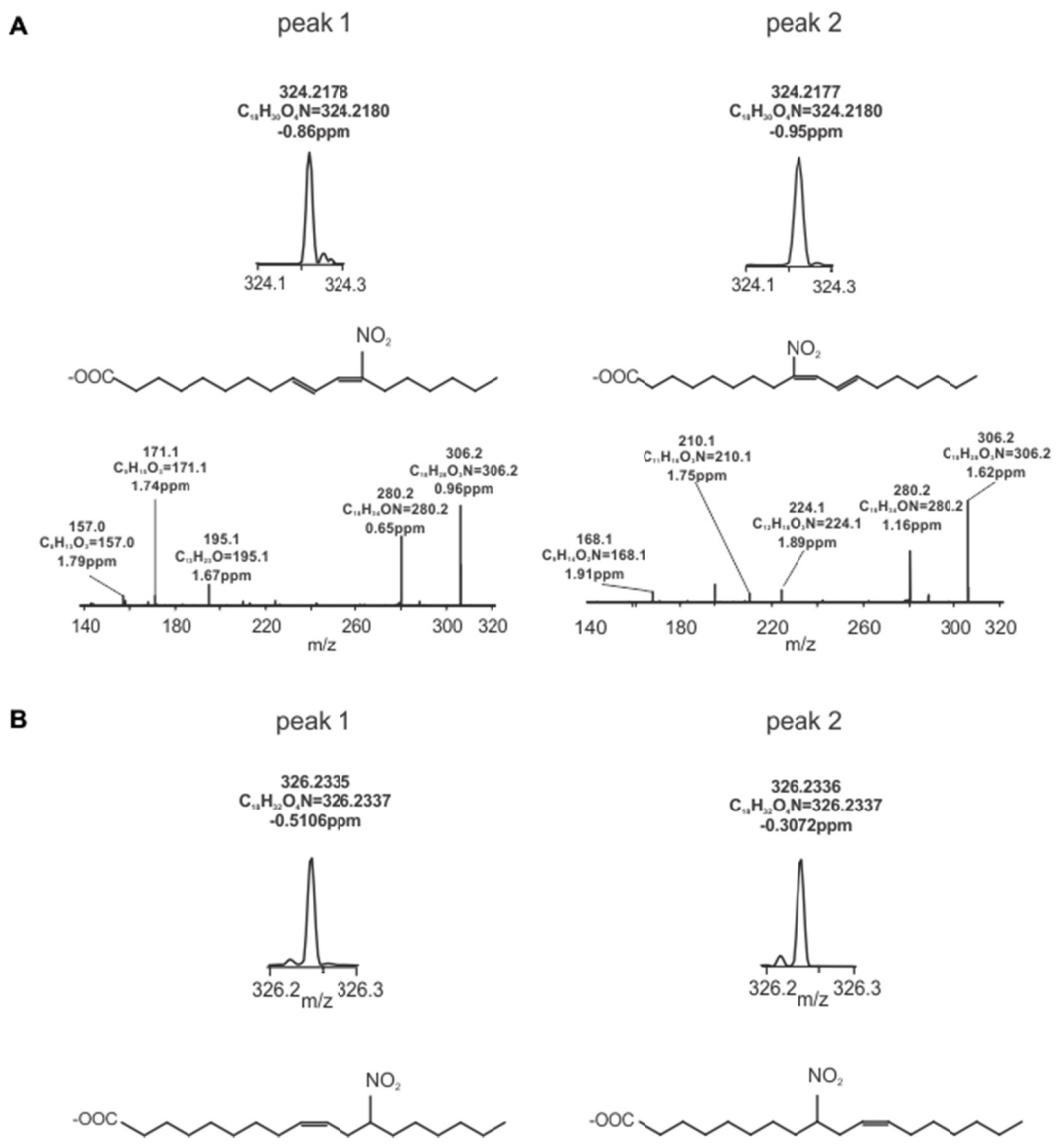

Figure S1: Structural confirmation for macrophage-generated NO_2-CLA and dihydro-NO_2-CLA. A) High-resolution LC-MS atomic composition determination, chemical structure and MS^2 fragmentation analysis for 12-NO_2-CLA (peak 1) and 9-NO_2-CLA (peak 2) respectively. B) High-resolution LC-MS atomic composition and chemical structure for dihydro-12-NO_2-CLA (peak 1) and dihydro-9-NO_2-CLA (peak 2) metabolites.

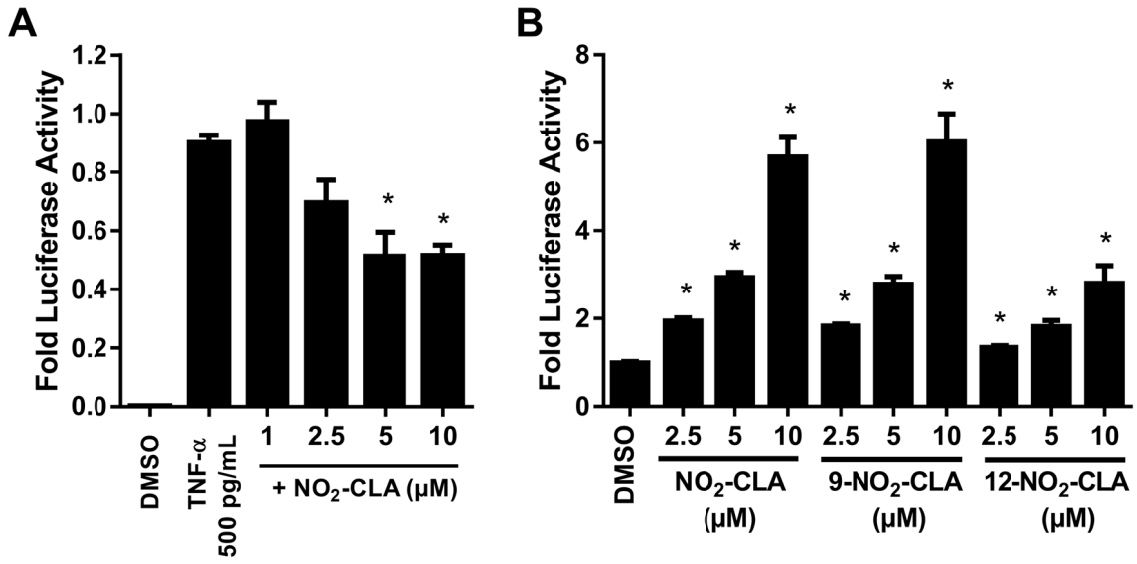

Figure S2: NO_2-CLA inhibits NF-κB-dependent gene expression and activates ARE/Nrf2-regulated transcription. A) Inhibition of NF-κB-dependent luciferase expression by NO_2-CLA in a HEK293 reporter cell line. B) NO_2-CLA stimulates Nrf2-dependent luciferase expression in a HepG2-based reporter cell line. Data are presented as mean ± SEM, * $p < 0.05$ vs. TNF-α alone (A) or vehicle control (B) as determined by one-way ANOVA and Dunnett's multiple comparison test (n=3-5).

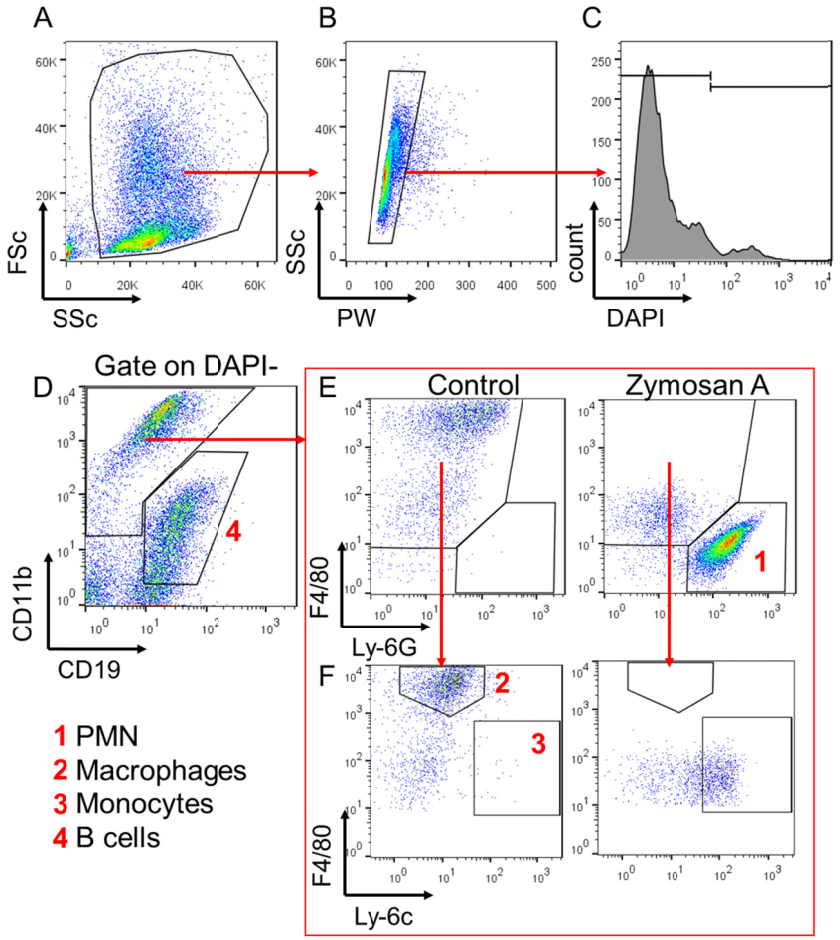

Figure S3: Gating strategy for flow cytometry analysis of peritoneal cell populations. A) Peritoneal cells were sequentially gated based on B) Sizing (Pulse width versus side scatter (SSc); C) Exclusion of death or dying cells (DAPI positive) and D) CD11b+, CD19- to exclude B-cells and other lymphocytes from cells of the monocytic lineage including monocytes, macrophages and PMN as described in the Experimental procedures section. E) Representative dot plots of PMN (Ly-6G^{+}) after gating on non-B-cells (defined in D as CD11b^{+}, CD19^{-}) in naïve peritoneal lavage (control) and zymosan-A challenged exudates (12h). F) Dot plots of macrophages (F4/80^{+}, Ly-6C^{-}) and monocytes (F4/80^{-}, Ly-6C^{+}) after gating on non-B-cells (defined in D as CD11b^{+}, CD19^{-}) in naïve peritoneal lavage (control) and zymosan-A induced inflammation (12h). Cell populations are identified as follows: 1 PMN: CD11b^{+}, CD19^{-}, F4/80^{-}, Ly-6G^{+}; 2 Macrophages: CD11b^{+}, CD19^{-}, F4/80^{high}; 3 Monocytes: CD11b^{+}, CD19^{-}, F4/80^{int}, Ly-6G^{-}, Ly-6c^{+}; 4 B cells: CD11b^{+}, CD19^{+}.

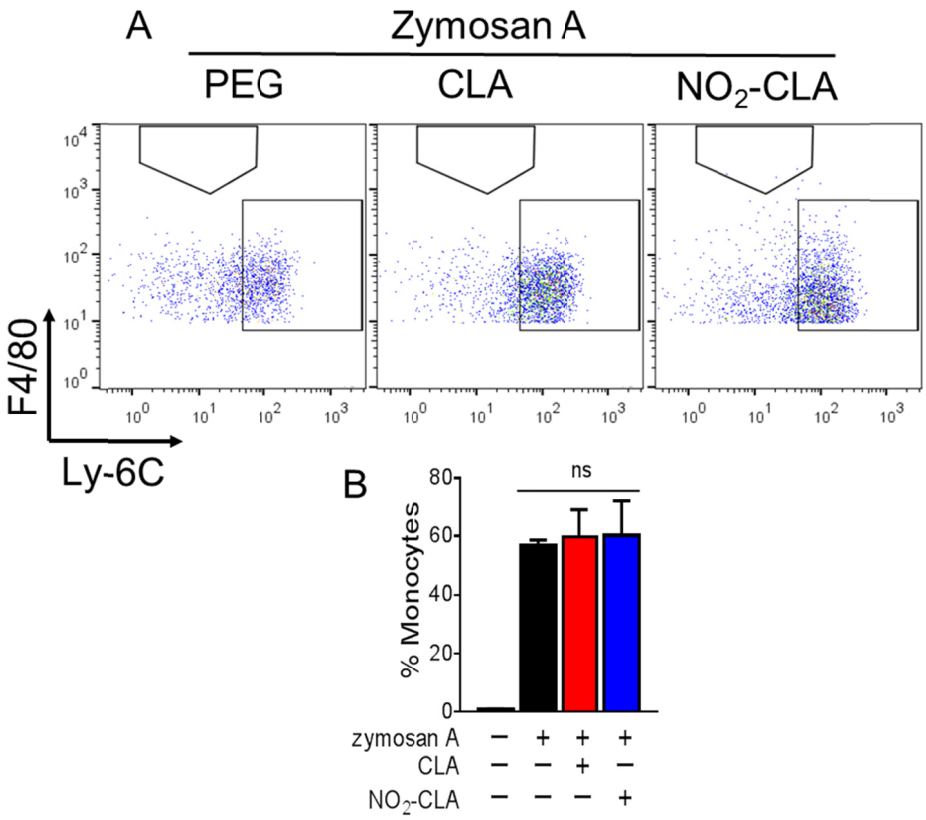

Figure S4: Monocyte recruitment is not altered by NO_2-CLA. A) Representative flow cytometry dot plot of exudate cells from either vehicle (PEG), CLA (2.5 mg) or NO_2-CLA (2.5 mg/kg) treated animals 12 hours after zymosan-A injection. B) At the maximal amplitude of PMN recruitment (12h), monocyte infiltration proceeding to a resolving stage is not altered by CLA or NO_2-CLA (n = 6).

Table S1: Primer sequences for RT-qPCR analysis

Gene	Species	Accession Number	Forward primer	Reverse Primer	Amplicon Size
18s RNA	H,R, M	X03205	5'-GGAAGGGCACCACCAGGAGT-3'	5'-TGCAGCCCCGGACATCTAAG-3'	
NOS 2	M	NM_010927	5'-GTTCTCAGCCCAACAATACAAGA-3'	5'-GTGGACGGGTCGATGTCAC-3'	127bp
IL6	M	NM_031168	5'-TAGTCCTTCCTACCCCAATTTCC-3'	5'-TTGGTCCTTAGCCACTCCTTC-3'	76bp
NQO 1	M	NM_008706	5'-AGGATGGGAGGTACTCGAATC-3'	5'-AGGCGTCCTTCCTTATATGCTA-3'	144bp
HO-1	M	NM_010442	5'-AAGCCGAGAATGCTGAGTTCA-3'	5'-GCCGTGTAGATATGGTACAAGGA-3'	100bp